*Article*

# Biogenesis of secretory immunoglobulin M requires intermediate non-native disulfide bonds and engagement of the protein disulfide isomerase ERp44

Chiara Giannone[1,2] (iD), Maria Rita Chelazzi[1,2] (iD), Andrea Orsi[1,2] (iD), Tiziana Anelli[1,2], Tuan Nguyen[3] (iD), Johannes Buchner[3] (iD) & Roberto Sitia[1,2,*] (iD)

## Abstract

Antibodies of the immunoglobulin M (IgM) class represent the frontline of humoral immune responses. They are secreted as planar polymers in which flanking $\mu_2L_2$ "monomeric" subunits are linked by two disulfide bonds, one formed by the penultimate cysteine (C575) in the tailpiece of secretory $\mu$ chains ($\mu_s$tp) and the second by C414 in the C$\mu$3. The latter bond is not present in membrane IgM. Here, we show that C575 forms a non-native, intra-subunit disulfide bond as a key step in the biogenesis of secretory IgM. The abundance of this unexpected intermediate correlates with the onset and extent of polymerization. The rearrangement of the C-terminal tails into a native quaternary structure is guaranteed by the engagement of protein disulfide isomerase ERp44, which attacks the non-native C575 bonds. The resulting conformational changes promote polymerization and formation of C414 disulfide linkages. This unusual assembly pathway allows secretory polymers to form without the risk of disturbing the role of membrane IgM as part of the B cell antigen receptor.

## Introduction

IgM antibodies are the first defense to infections in humoral immune responses (Boes, 2000). As in all antibody classes, two heavy (H) and two light (L) chains assemble to form $\mu_2L_2$ subunits, often called "monomers" in the immunological jargon (Wiersma & Shulman, 1995). In B cells, IgM antibodies are produced in a membrane-bound form ($\mu_m$) and assembled with accessory molecules to serve as antigen receptors (BCR) (Reth, 1989). Upon antigen stimulation, B cells shift to the production of secreted IgM polymers that act as effector molecules (Sidman, 1981; Alberini *et al*, 1987). H chains differing in their C-terminal regions ($\mu_m$ and $\mu_s$) are produced by alternative RNA processing (Alt *et al*, 1980; Kehry *et al*, 1980; Rogers & Wall, 1980). $\mu_m$ contains a stretch of hydrophobic amino acids that allows membrane insertion, while $\mu_s$ possesses a highly conserved peptide extension of 18 amino acid residues (Davis & Shulman, 1989; Sitia *et al*, 1990; Pasalic *et al*, 2017). This tailpiece ($\mu_s$tp) mediates the formation of planar IgM polymers (Li *et al*, 2020). Multivalence confers high avidity for antigen and compensates for the low affinity of each monomer, whose variable regions are generally in the germline configuration (Thomas & Morgan-Capner, 1990).

Ig secreting cells produce an additional protein, the J chain (Chapuis & Koshland, 1974). A single J chain is assembled with five $\mu_{s2}L_2$ subunits (Mihaesco *et al*, 1973). J-containing pentamers bind to the polymeric Ig receptors, which mediate transcytosis across epithelia for mucosal immunity (Brandtzaeg & Prydz, 1984). In the absence of J chains, six $\mu_{s2}L_2$ subunits associate into hexamers (Fig 1A) (Cattaneo & Neuberger, 1987; Hendrickson *et al*, 1995; Brewer & Corley, 1997; Källberg & Leanderson, 2006), which are particularly efficient in activating complement-dependent cytotoxicity (Feinstein & Munn, 1969; Davis *et al*, 1988; Taylor *et al*, 1994).

Several inter-chain disulfide bonds confer stability to IgM polymers (Milstein *et al*, 1975; Wiersma & Shulman, 1995). C337 in the C$\mu$2 domain links the two $\mu$ chains within one $\mu_2L_2$ subunit (Fig 1B). Key inter-subunit bonds are formed by C575, a conserved residue occupying the penultimate position in the $\mu_s$tp (Davis & Shulman, 1989; Sitia *et al*, 1990); C414 in the C$\mu$3 domain forms a second inter-subunit bond. The presence of two bonds that link the C$\mu$3 and C$\mu$4 domains of flanking $\mu_{s2}L_2$ subunits (Fig 1A) confers

1 Division of Genetics and Cell Biology, Università Vita-Salute IRCCS Ospedale San Raffaele, Milano, Italy
2 Vita-Salute San Raffaele University, Milan, Italy
3 Department Chemistry, Technical University Munich, Garching, Germany
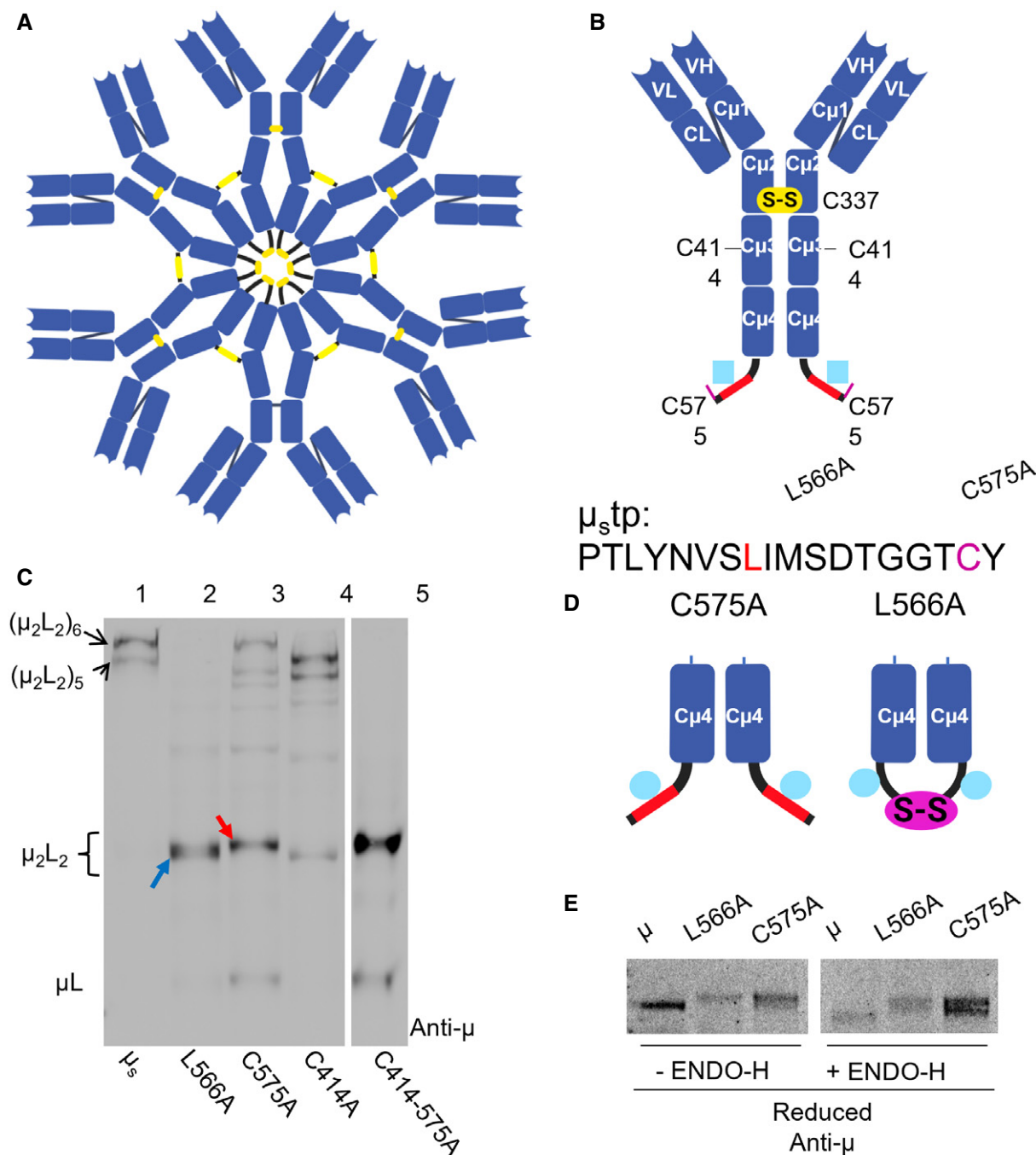*Corresponding author. Tel: +39 0226434722; E-mail: sitia.roberto@hsr.it

**Figure 1. Secretion of μ_{s2}L_2 subunits with different electrophoretic mobilities upon mutation of key μ_stp residues.**

A  Schematic representation of an IgM hexamer. Six μ_{s2}L_2 "monomeric" subunits are arranged in planar polymers stabilized by inter-subunit disulfide bonds via C414 in the Cμ3 and C575 in the μ_stp (yellow lines).

B  Schematic representation of an IgM "monomer". C337 links two μ chains within a μ_{s2}L_2 subunit. The conserved high mannose N-glycans which become inaccessible to Golgi enzymes in polymers are depicted as blue squares, while the hydrophobic stretch is in red. The amino acidic sequence of the murine μ_stp is shown in the lower panel. C575 is highlighted in purple and the hydrophobic residue L566 in red.

C  Aliquots of the supernatants of the indicated HEK293T transfectants (all expressing λ chains) were resolved under non-reducing conditions and blotted with anti-μ antibodies. Wild-type μ_s chains are secreted only as pentamers and hexamers, while mutants lacking C575 release mostly μ_{s2}L_2 subunits (indicated with a red arrow) as does the double C414A-C575A. L566A releases instead mainly μ_{s2}L_2 subunits of faster migration (blue arrow). C414 mutants release no hexamers, but smaller assemblies, including fast migrating μ_{s2}L_2 subunits.

D  Schematic view of the organization of μ_2L_2 subunits secreted by L566A and C575A mutants. For simplicity, only the tailpieces and the last constant domain (Cμ4) are shown. The L566A mutant has a disulfide bond that links two C575 in the same subunit. The open conformation of the tailpieces in C575A likely causes its slow electrophoretic mobility. The N563-glycans are processed in both mutants (see E below).

E  Aliquots of the supernatants were treated with or without Endo-H and electrophoresed under reducing conditions. The blot was decorated with anti-μ antibodies. N563-glycans acquire Endo-H resistance in μ_sL566A and μ_sC575A, but remain largely sensitive in wild-type μ_s.

rigidity to IgM polymers, facilitating complement fixation (Davis & Shulman, 1989; Brewer & Corley, 1997; Czajkowsky & Shao, 2009). However, C414 does not form inter-subunits bonds in membrane IgM, as only $\mu_{m2}L_2$ are found in BCRs (Venkitaraman *et al*, 1991).

Structural insights on the structure of this complex molecule have been obtained by X-ray crystallography and NMR—for individual IgM constant domains (Müller *et al*, 2013), negative stain electron microscopy (EM)—for the Fc portion of secreted IgM polymers (Hiramoto *et al*, 2018), and more recently by cryo-EM for J chain containing pentamers bound to the secretory component (Li *et al*, 2020). The latter structure reveals that the $\mu_s$tps covalently connect distinct subunits in the oligomer via disulfide bonds. In addition, the beta strands formed by residues 562-568 in the $\mu_s$tp are part of an antiparallel beta sandwich at the core of the polymer. Interestingly, five of these extremely conserved hydrophobic residues (Y562, L564, L566, I567, and M568) are essential for polymerization (Pasalic *et al*, 2017). Also, invariable in the $\mu_s$tp is a mannose-rich glycan linked to N563 that contributes to limiting the size of polymers (Giannone *et al*, 2017).

C575 plays an important role in mediating assembly, retention, and degradation of unpolymerized subunits (Fra *et al*, 1993). Secretion of incompletely assembled IgM subunits is prevented by thiol-mediated quality control (Tempio & Anelli, 2020). A key role is played by ERp44, a PDI family member that forms mixed disulfides with C575 on the $\mu_s$tp (Anelli, 2003). Also, ERGIC-53, a polymeric lectin that cycles in the early secretory compartment in association with ERp44 (Tempio *et al*, 2021) and binds the N563-glycans (Cortini & Sitia, 2010), promotes IgM polymerization (Anelli *et al*, 2007). Thus, the $\mu_s$tp contains most of the information dictating the biogenesis of IgM polymers (Pasalic *et al*, 2017). However, the cellular mechanisms that allow the formation of these elegant structures are still undefined.

We have shown previously that C575 plays an essential role in the assembly of polymeric structures *in vivo* as well as *in vitro* covalently linking two $\mu_s$ chains from different subunits (Sitia *et al*, 1990; Pasalic *et al*, 2017). Here, we investigated how C575 triggers polymerization. Intuitively, one would predict that mechanisms are in place to prevent the formation of disulfide bonds between two C575 within the same $\mu_{s2}L_2$ subunit. In fact, our results reveal that, surprisingly, such a non-native disulfide bond is essential for the efficient polymerization of secretory IgM.

# Results

### A non-native disulfide bond linking C575 in the same subunit during IgM polymerization

To investigate the mechanisms of IgM polymerization, we co-expressed nitrophenol (NP)-specific secretory $\mu$ ($\mu_s$) variants and $\lambda$ chains in different cell types (Neuberger *et al*, 1984). As shown in Fig 1C, HEK293T cells secreted high-molecular-weight complexes likely corresponding to $(\mu_{s2}L_2)_6$ "hexamers" and, in smaller amounts, $(\mu_{s2}L_2)_5$ "pentamers" (Hiramoto *et al*, 2018; Li *et al*, 2020). As previously described (Sitia *et al*, 1990), alanine replacement of C575 induced secretion of mostly $\mu_{s2}L_2$ "monomers": Few covalently linked hexamers were formed via C414 in C$\mu$3 (Fig 1C, lane 3). In the absence of C414, instead, abundant pentamers and

tetramers and few monomers, but virtually no hexamers were secreted, confirming the leading role of C575 in triggering polymerization (Fig 1C, lane 4). As expected, only $\mu_{s2}L_2$ monomers were secreted upon replacement of both C414 and C575 (Fig 1C lane 5). Noteworthy, a similar phenotype was observed upon replacement of hydrophobic residues in the $\mu_s$tp such as L566A (Fig 1C, lane 2), in line with previous results (Pasalic *et al*, 2017). Unexpectedly, therefore, reducing the overall hydrophobicity of the $\mu_s$tp drastically reduced the propensity of C414 and C575 to form inter-subunit bonds.

We noticed that the $\mu_{s2}L_2$ species secreted by the L566A variant displayed faster electrophoretic mobility than C575A monomers (compare blue and red arrows in Fig 1C, lanes 2 and 3). A similar pattern was observed for other hydrophobic mutants (Pasalic *et al*, 2017). Differential glycan processing was not the cause of the different gel mobility, as their complete removal by PNGase-F did not abolish the differences between L566A and C575A (Fig EV1C). The N563-glycans are sensitive to Endo-H in wild-type IgM polymers, because polymerization hinders them from Golgi processing enzymes (Cals *et al*, 1996). In contrast, L566A and C575A were largely resistant to Endo-H, confirming that both mutants proceed through the Golgi with accessible N-glycans, such as C575A (Fig 1E) as does the double mutant C575AC414A (Fig EV1B).

Having excluded glycan processing, the faster migration of L566A could be explained by the formation of an intra-subunit C575-C575 disulfide bond. Such a linkage would secure the two $\mu_s$tps within the same subunit together, yielding a more compact conformation of the Fc region, with faster electrophoretic mobility (Fig 1D). Accordingly, unassembled wild-type and mutant $\mu$ chains migrated similarly upon deglycosylation with PNGase-F and complete reduction with DTT (Fig EV1D). Importantly, also mild reduction under non-denaturing conditions abolished the mobility differences (Fig EV1E). Thus, an intra-monomeric disulfide bond between two C575 is formed when one of the $\mu_s$tp hydrophobic amino acids is missing (Fig 1D). Interestingly, this compact conformation limits also the reactivity of C414 (compare lanes 3 and 4 in Fig 1C). Taken together, these results identify a non-native covalent linkage that involves C575 in the tailpieces of $\mu_{s2}L_2$ subunits and suggest that hydrophobic cues present in the $\mu_s$tps govern disulfide bond rearrangements during IgM biogenesis.

### C575 forms non-native intra-subunit disulfides also in cells of the B lineage

To confirm that the formation of hyperoxidized $\mu_{s2}L_2$ subunits containing a C575 disulfide ($\mu_{s2}L_2C575_{ox}$) is part of the physiological polymerization process, we analyzed J558L plasma cells expressing endogenous Ig-$\lambda$ chains transfected with wild type or C575A $\mu_s$ (Fig 2A). A faster migrating $\mu_{s2}L_2$ band was detectable (blue arrow) in the lysates of myeloma transfectants producing wild-type $\mu_s$ but not the C575A mutant. The mobility shift was not abolished upon removal of the sugars by PNGase F (compare the two right lanes in panel A), implying different $\mu_s$tp conformations.

The presence of $\mu_{s2}L_2C575_{ox}$ was confirmed by nano-scale liquid chromatographic electrospray ionization tandem mass spectrometry (nLC-ESI-MS/MS). $\mu_{s2}L_2$ subunits were affinity purified from the lysates of B1.8, a murine hybridoma secreting NP-specific IgM (Reth *et al*, 1978) and analyzed by sequential alkylation as described in Fig 2B. In this assay, $\mu_{s2}L_2C575_{ox}$ present in cells would yield
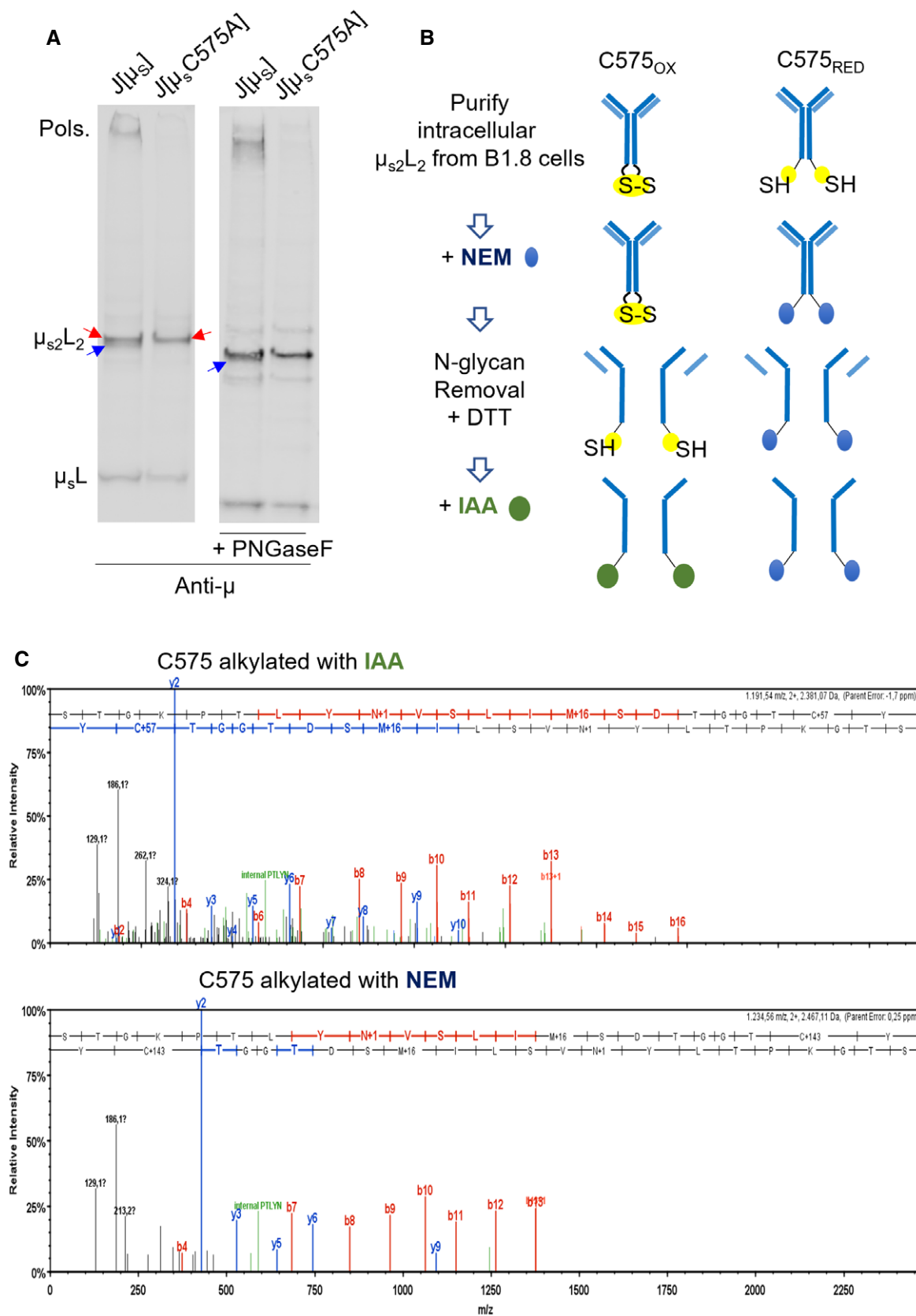
Chiara Giannone et al

Figure 2.

◀

**Figure 2.   Formation of $\mu_{s2}L_2$-C575$_{OX}$ intermediates in myelomas and hybridomas.**

A      Aliquots of the lysates from J558L transfectants expressing wild-type $\mu_s$ or $\mu_s$C575A chains were resolved under non-reducing conditions before or after removal of N-glycans by PNGase-F. Blots were decorated with anti-$\mu$ antibodies. Blue and red arrows point to the closed (oxidized) and open $\mu_{s2}L_2$ species respectively.

B, C   Intracellular $\mu_{s2}L_2$ species purified from the murine hybridoma B1.8 were subjected to the sequential alkylation protocol described in panel B and analyzed by mass spectrometry (panel C). In the MS/MS spectrum, Y and B ions are shown in blue and red, respectively.

peptides with C575 bound to iodoacetamide (IAA), as the residues would be unavailable to N-ethyl maleimide (NEM) during lysis. IAA would be bound after reduction and alkylation *in vitro*. In contrast, NEM binding to peptides would reflect an accessible thiol or thiolate groups at lysis. The detection of both species in similar amounts (Fig 2C) demonstrated that $\mu_{s2}L_2$C575$_{ox}$ is not an artifact observed in non-lymphoid cells. Fragmentation table of the reported mass spectrometry analyses is reported in Fig EV2A. Considering that NEM binding could be partly reversible, the experiment was repeated inverting the order of alkylants, to confirm that C575 was indeed oxidized at the moment of lysis. Thus, IAA was added before detergent lysis to irreversibly block cysteine thiols, and NEM used after reduction with DTT to label cystines (Fig EV2B). Also in this case, C575 was found bound to both IAA and NEM (Fig EV2B), making the possibility of post-lytical modifications unlikely. Thus, C575 forms non-native, intra-subunit disulfide bonds also in IgM secreting plasma cells.

### Formation of intra-subunit C575 bonds correlates with the extent of IgM secretion

To further investigate the role of C575 non-native disulfide bond and to test its involvement in IgM polymerization, we analyzed cells from the inducible I.29$\mu^+$ B lymphoma. When grown in the absence of mitogens, these cells express membrane IgM on their surface and degrade most secretory $\mu$ chains. Upon stimulation with lipopolysaccharide (LPS), however, they lose their BCR and switch toward IgM secretion (van Anken *et al*, 2003; Cenci *et al*, 2006).

We reasoned that if the formation of non-native C575 intra-subunit disulfides was indeed a step in IgM polymerization, then $\mu_{s2}L_2$C575$_{ox}$ should be more abundant upon LPS stimulation, when I.29$\mu^+$ cells begin to secrete IgM. To avoid confusion with membrane $\mu_{m2}L_2$, we fractionated lysates in the presence of Triton X-114 (Fig 3A), which allows separation of membrane (detergent fraction) from soluble proteins (aqueous fraction). As expected, 4 days after LPS stimulation, large amounts of polymers were present only in the soluble fraction, while membrane-bound IgM markedly decreased in the detergent fraction. Noteworthy, only $\mu_{m2}L_2$ species were detected in the detergent fraction. Therefore— unlike in secreted polymers—C414 does not form disulfide bonds between subunit in membrane IgM.

Next, the Triton X-114 soluble material obtained by I.29$\mu^+$ cells treated with or without LPS was fractionated by density sucrose gradients. The fractions enriched in $\mu_{s2}L_2$ subunits and devoid of polymers and were subjected to a two-step alkylation protocol (Fig 3B) to assess the redox state of C575. In this case, the second step entailed alkylation with 4′-acetamido-4′-maleimidylstilbene-2,2′-disulfonic acid (AMS), the binding of which increases the protein mass by about 500 Da. With this strategy, alkylation with AMS implies that C575 was protected from NEM during cell lysis

and hence oxidized. As can be seen in Fig 3C, clearly, a considerable fraction of $\mu_s$ chains isolated from LPS-treated cells migrated more slowly, suggesting that C575 oxidation increased when IgM secretion ensues. Further quantitative analyses by nLC-ESI-MS/MS confirmed that the abundance of intra-subunit C575 disulfides in I.29$\mu$ + cells correlates with IgM polymerization. At day 3, the fraction of oxidized C575 doubled compared with unstimulated cells (Fig 3D). Notably, an opposite trend was detected for C414 after induction with LPS. Contrary to C575, the fraction of oxidized C414 was decreased by twofold at day 3 of LPS stimulation, further underscoring the specificity of the redox modifications described.

### ERp44 attacks oxidized C575 and favors IgM polymerization

The above data indicated that IgM assembly entails an unexpected intermediate in which a non-native disulfide bond covalently links two $\mu_s$tps within the same subunit. This species can no longer participate in the covalent assembly of IgM oligomers. However, only small amounts of unpolymerized IgM are secreted, implying that the non-native disulfide bond is isomerized into inter-subunit linkages. We have shown previously that ERp44 prevents the secretion of unpolymerized IgM (Anelli, 2003; Anelli *et al*, 2007). ERp44 uses a cysteine in its active site (C29) to form mixed disulfides with its clients (Tempio & Anelli, 2020). Recent findings indicate that monomeric ERp44 preferentially attacks non-native or regulatory disulfides when in suitable pH and ionic conditions (Yang *et al*, 2016; Watanabe *et al*, 2017). To test whether ERp44 targets the non-native disulfide bond in $\mu_{s2}L_2$C575$_{ox}$, we generated ERp44$^{KO}$ HeLa cells by CRISPR and reconstituted them with different Halo-tagged ERp44 variants (Fig 4). ERp44$^{KO}$ HeLa secreted mainly $\mu_{s2}L_2$ subunits (panel A, see blue arrow), confirming the key role of ERp44 in IgM quality control (Anelli, 2003). Only traces of polymers were detectable in the supernatants. The expression of wild-type ERp44 prevented the secretion of $\mu_{s2}L_2$ subunits and promoted polymerization (Fig 4A, see black arrow). Also, an ERp44 mutant unable to bind zinc (3HA) (Watanabe *et al*, 2019) and mostly localized in the Golgi (Sannino *et al*, 2014), efficiently retained intracellularly IgM intermediates (Fig EV3). In contrast, neither secretion nor polymerization was affected by ERp44 mutants lacking the active cysteine or the RDEL sequence for client binding and ER retrieval (C29S and ΔRDEL), respectively (Fig EV3 and Fig 4). ERp44ΔRDEL formed very few covalent complexes with IgM (Fig 4A and B, black asterisks, Fig EV4B), suggesting that client binding by ERp44 could be promoted by interactions with KDEL receptors.

ERp44 retained also the L566A mutant, although with much lower efficiency than wild-type $\mu_{s2}L_2$ (Figs 4A and EV4A). However, it failed to induce polymerization of the mutant (Fig 4B). Covalent complexes between L566A and ERp44, likely containing a $\mu_2L_2$ and one or more Halo-ERp44 molecules, were detected serologically in ERp44$^{KO}$ cells after co-expression of the two proteins (Fig 4C). The
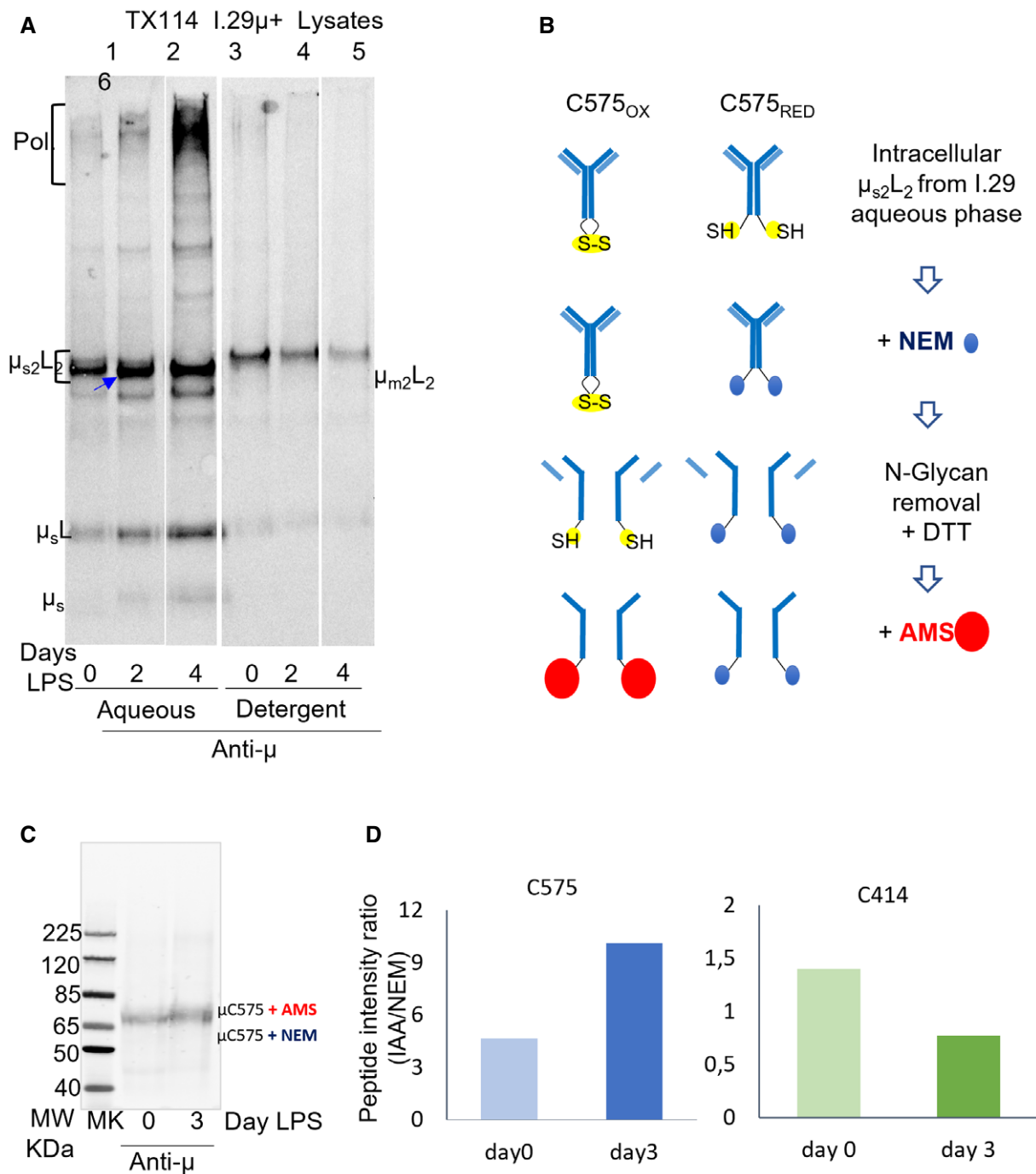
Chiara Giannone et al

**Figure 3. The levels of $\mu_{s2}L_2$-C575$_{OX}$ intermediates correlate with IgM secretion.**

A I.29$\mu$+ B lymphoma cells were treated with LPS to induce differentiation toward IgM secretion. At the indicated times, cells were lysed in Triton X-114 to separate soluble and integral membrane proteins (aqueous and detergent phases, respectively). Aliquots from the two phases were resolved electrophoretically, and the blot was decorated by anti-$\mu$ antibodies. The blue arrow points at a band likely corresponding to $\mu_{s2}L_2$C575$_{OX}$, the intensity of which increases upon LPS stimulation.

B After sucrose gradient fractionation, $\mu_{s2}L_2$ extracted from the aqueous phases of I.29$\mu$+ cells were sequentially alkylated with NEM and AMS as described in the scheme.

C $\mu$-chains with oxidized C575 bind AMS after reduction and migrate more slowly than those which were reduced at the time of lysis and hence alkylated by NEM.

D The bar graphs show the levels of C575 and C414 oxidation, expressed as the ratio between IAA and NEM modified peptides. These analyses confirm the increase of $\mu_{s2}L_2$C575$_{OX}$ species during B-cell differentiation observed biochemically in panels A and C.
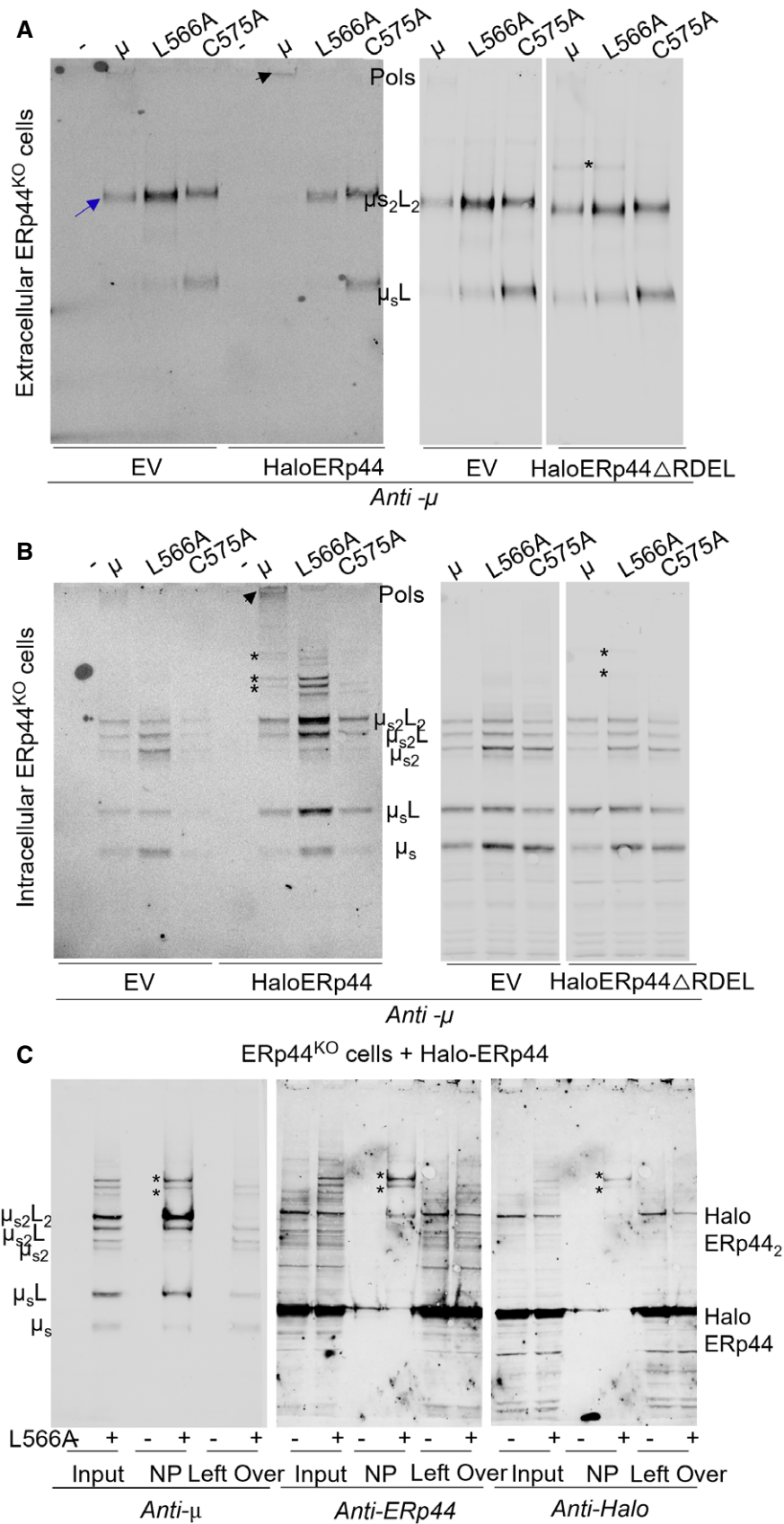
**Figure 4.**

◄

**Figure 4.  ERp44 attacks the non-native disulfide bond formed by two C575 within single subunits.**

ERp44$^{KO}$ HeLa cells expressing Ig-λ chains were transfected with wild type (μ), L566A or C575A mutant μ$_s$ chains and Halo-ERp44, or Halo-ERp44ΔRDEL, as indicated. Empty vectors (- or EV) served as controls.

A  Aliquots from the spent media (Extracellular) were blotted under non-reducing conditions and decorated with anti-μ antibodies. The blue arrow points at the faster migrating μ$_{s2}$L$_2$ released by cells expressing wild-type μ$_s$ or L566A chains. Expression of Halo-ERp44 restores C575-dependent retention, and wild-type μ$_s$ are secreted only as polymers (black arrow). Traces of covalent Halo-ERp44-μ$_2$L$_2$ complexes (black asterisks) are detected in the media of cells expressing Halo-ERp44ΔRDEL and μ$_s$ or L566A. The slightly faster mobility of μ$_{s2}$L$_2$ and μ$_s$L complexes released by cells expressing ERp44ΔRDEL suggests that the latter inhibits processing of the N563 glycan, likely hindering it to the Golgi enzymes upon non-covalent binding.

B  The corresponding cell lysates are shown in this panel. The short black arrow points at the polymers formed in ERp44$^{KO}$ HeLa cells upon expression of wild-type Halo-ERp44. The black asterisks indicate covalent complexes that this transgene forms with C575 containing μ$_2$L$_2$. Traces of intracellular μ$_{s2}$L$_2$-ERp44ΔRDEL complexes are visible in μ$_s$ and L566A but absent from C575A expressing cells.

C  Lysates of the ERp44$^{KO}$ transfectants were precipitated with NP-sepharose, resolved under non-reducing conditions and the blot decorated sequentially with anti-μ, anti-ERp44 or anti-Halo. The two black asterisks point at bands corresponding to covalent complexes containing μ$_{s2}$L$_2$ and endogenous or Halo-tagged ERp44.

Data information: All membranes were decorated with anti-μ antibodies. Black roundish spots seen in the left panels are artifacts that formed during blotting procedures and signal acquisition.

absence of similar complexes with the mutant C575A (Fig EV5B) and their formation with wild-type μ$_s$ (Fig EV5A) confirmed that ERp44 binds preferentially C575 in the tailpiece. Despite its interactions with ERp44, the L566A mutant did not form polymers. Moreover, the secreted L566A μ$_{s2}$L$_2$ displayed the fast mobility typical of subunits with oxidized C575 (Fig 4A), which was found as oxidized by mass spectrometry analyses (Fig EV6). Taken together, these findings indicated that the non-native C575 bond is attacked by ERp44. ERp44 inhibits secretion of μ$_{s2}$L$_2$C575$_{ox}$ and promotes their polymerization. Most L566A mutants escape ERp44-dependent quality control and are secreted as μ$_{s2}$L$_2$C575$_{ox}$ subunits, although ERp44 can recognize its non-native disulfide. The conserved hydrophobic cues in the μ$_s$tp may thus make the non-native bond less stable and/or favor ERp44 binding, facilitating its isomerization into inter-subunit linkages.

Abundant μ$_s$L subunits were detected in the supernatants of ERp44$^{KO}$ transfectants that express mutants lacking C575 (Fig EV7B). These μ$_s$L species were barely detectable in C414A mutant (see Fig EV7B). Also, the compactness of the μ$_{s2}$L$_2$ bands released by these mutants argues in favor of the presence of two intra-subunit covalent linkages, involving C337 in the Cμ2 and C575 in the μ$_s$tp. Thus, the non-native C575 bonds seem to favor the formation of both C414-C414 inter-subunit and C337-C337 intra-subunit disulfide bonds.

**An obligatory step in IgM polymerization**

To determine whether these non-native disulfides were an obligatory step in IgM biogenesis, or rather part of a parallel or off-pathway, we took advantage of the possibility of co-expressing differently tagged μ chains (Fig 5). The rationale of the experiment was that if the intra-monomeric bond was an essential step, hybrid μ$_{s2}$L$_2$ subunits containing only one C575, should not be able to efficiently associate into (μ$_{s2}$L$_2$)$_2$ species connected by inter-subunit C575-C575 linkages (Fig 5A). Thus, we co-expressed wild-type μ$_s$ and a C575A variant extended with a Halo-tag to allow easy discrimination of the two chains. To eliminate any confounding effects due to C414-dependent associations, we replaced it with alanine (C414A). As expected, abundant polymers and some μ$_{s2}$L$_2$ were secreted by cells expressing μ chains with a cysteine at position 575 but lacking C414 (Fig 5B lane 5). In contrast, Halo-μC575A was secreted only as μ$_{s2}$L$_2$ and μ$_s$L subunits (lane 4). Notably, two additional bands were detectable in the lysates of cells co-expressing both wild-type and C575 μ$_s$ chains (lane 3). These bands displayed the intermediate mobility and immunoreactivity expected for a hybrid μ$_s$C575-Halo-μ$_s$A575L$_2$. Even if they contained a C575 in one of the two μ$_s$tps, however, they did not form higher order assemblies. Their identity was confirmed by precipitation with sepharose-conjugated NP, which binds only properly folded μ$_s$L assemblies (right panel in Fig 5B, lane 9). Clearly, the hybrid-μ$_{sC575}$-Haloμ$_{sA575}$L$_2$ species did not polymerize further via the available C575. Thus, in cells overexpressing different μ chains, μ$_s$L formed hybrid dimers, albeit with low efficiency. Importantly, the single C575 in these hybrids showed limited reactivity, and no polymeric intermediates could be detected.

To determine whether ERp44 can bind the unpaired C575 in hybrid μ$_{s2}$L$_2$ subunits (Fig 5C) Halo-ERp44 was co-expressed in ERp44$^{KO}$ cells producing both μ$_s$C575 and Halo-μ$_s$A575. Covalent complexes were observed, as expected, between μ$_s$C575$_2$L$_2$ and Halo-ERp44 (Fig 5C, lanes 4 and 10, black asterisks), but no bands

**Figure 5.  Formation of intra-subunit C575 bonds is needed for efficient polymerization.** ►

A  Schematic view of the mutants generated to evaluate the functional role of the C575 intra-subunit bonds. HEK293T cells expressing λ chains were transfected with μHaloC575A-C414A (HC575A, depicted in red in the figure), μC414A (μ, in blue) or both mutants together.

B  To selectively label intracellular HC575A, cells were treated with 1 nM Halo-tag TMR Direct Ligand for 24 h. The left panel shows aliquots of the lysates of the indicated transfectants, resolved under non-reducing conditions, and decorated with anti-λ antibodies. In the two right panels, samples were precipitated with NP-Sepharose and electrophoresed under non-reducing conditions. The signal for the Halo-tag TMR was checked directly in the gel. The arrows point at the various assemblies between μ, HC575A and λ chains.

C  The experiment shown aims to determine whether ERp44 can bind also to a single C575, or rather to non-native bonds. Aliquots of the lysates from the indicated ERp44$^{KO}$ transfectants were precipitated with NP-Sepharose, resolved under non-reducing conditions and the blot decorated with anti-λ antibodies or anti-ERp44 as indicated. Black asterisks point to covalent complexes of Halo-ERp44 with μ$_{s2}$L$_2$.
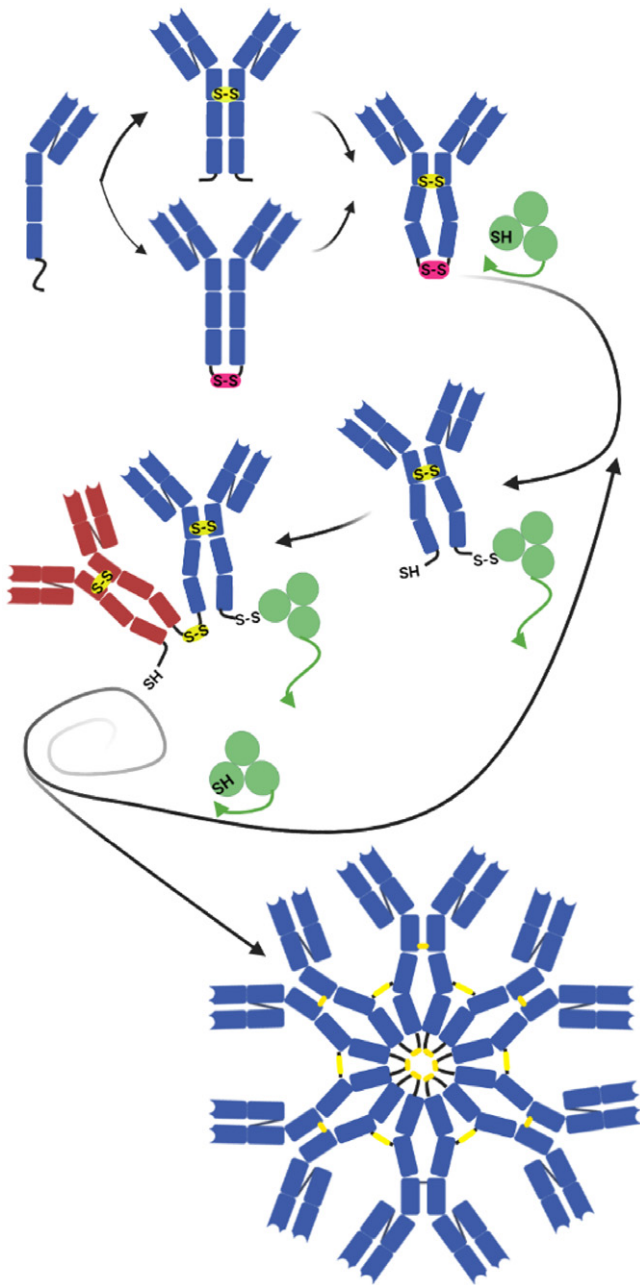
Figure 5.

**Figure 6. A model for IgM polymerization.**

$\mu_s$L (in blue) dimerization likely proceeds via C337 in C$\mu$2 (top arrow) though C575 intra-subunit bonds (in pink) may favor covalent binding via C337 (in yellow). Compact $\mu_{s2}L_2C575_{OX}$ subunits are then formed which are attacked by ERp44 (depicted in green). Polymerization proceeds by sequential recruitment of mixed ERp44- $\mu_{s2}L_2$ complexes, until fully oxidized hexamers are formed. A reduced ERp44 is released at each step. It is also possible that oxidized $\mu_{s2}L_2$ subunits (in red) bind directly to an ERp44- $\mu_{s2}L_2$ complex.

were detected that could correspond to complexes between Halo-ERp44 and hybrid monomers (Fig 5C, lanes 6 and 12). These results suggest that a free C575 does not react stably with ERp44 (Fig 5C) and the non-native intra-subunit bond is important for ERp44 and binding and subsequent polymerization. Moreover, our data suggest

that $\mu_s$L can assemble also post-translationally, when overexpressed in non-lymphoid cells. In B cells, few $\mu_s\mu_mL_2$ were seen (Fig 3), suggesting that co-translational dimerization prevails, and/or hybrid species promptly rearrange.

## Discussion

Considering the structure of IgM, one would think that for polymerization to occur, the two C575 present in a single $\mu_{s2}L_2$ subunit should never form intra-subunit bonds, as this would impede their pairing with residues from an adjacent subunit or a J chain that stabilize native oligomers (Hiramoto et al, 2018; Li et al, 2020). The abundance of non-native, intra-subunit disulfide bonds involving C575 in IgM secreting cells came hence as a great surprise. Their presence was confirmed by rigorous biochemical and mass spectrometry analyses. Importantly, their abundance correlated with the efficiency of IgM polymerization in differentiating B cells. Cells secreting wild-type IgM contain similar amounts of reduced $\mu_{s2}L_2$ and compact $\mu_{s2}L_2C575_{OX}$, but they release only pentamers and hexamers. In contrast, predominantly $\mu_{s2}L_2C575_{OX}$ subunits are secreted by cells that lack ERp44.

In our model, the proximity of the two $\mu_s$tps in newly made $\mu_{s2}L_2$ species could be the reason of the formation of the non-native intra-subunit C575 disulfide bond. The bond is then attacked by ERp44 and a covalent complex is formed between a C575 in $\mu_{s2}L_2$ and C29 of ERp44 (Fig 6). The interaction may occur in the ER or—perhaps more likely—in downstream compartments, where the lower pH and higher zinc concentration induce rearrangements of the ERp44 C-tail (Watanabe et al, 2019). Exposure of C29 can favor covalent client binding at an unfavorable pH. Reduced formation of the native, inter-subunit C575 disulfide releases reduced ERp44, which is then ready for another cycle of interaction making its function in IgM assembly catalytic.

ERp44 probably induces conformational changes in $\mu_{s2}L_2$, favoring the exposure and/or reactivity of C414. Inter-subunit bonds via C414 stabilize nascent assemblies, favoring their growth in a planar configuration until hexameric structures are formed (Wiersma & Shulman, 1995). Lack of C414 linkages may explain the few pentamers formed in the absence of J chains in HEK cells.

Notably, C575 oxidation is essential also to initiate polymerization of purified C$\mu$4-tp fragments in vitro. When C575 is replaced or alkylated, C$\mu$4-tp fragments remain in the monomeric state (Pasalic et al, 2017), implying that the C575 bond causes structural changes in the $\mu_s$tp and/or in the C$\mu$4 domain that trigger oligomerization. These changes require the presence of four hydrophobic residues in the $\mu_s$tp. Replacing L566 (or any other of them) inhibits polymerization of covalent C$\mu$4-tp dimers in vitro. In living cells, the constrains imposed by the local hydrophobicity make the intra-subunit bond more accessible to ERp44, whose CRFS active motif recognizes preferentially non-native disulfides (Yang et al, 2016; Hampe et al, 2017; Watanabe et al, 2017). In its absence, ERp44[KO] cells massively secrete compact $\mu_{s2}L_2C575_{OX}$. Expression of active ERp44 rescues retention and allows polymerization. Thus, ERp44 attacks the non-native bond in $\mu_{s2}L_2C575_{OX}$, triggering polymerization. ERp44 binds also to $\mu_{s2}L_2C575_{OX}$ in which the $\mu_s$tp hydrophobic mutants are mutated. However, it neither retains them completely, nor does it induce their polymerization. The absence of hydrophobic cues could

© 2021 The Authors

make it more difficult for individual subunits to get close to each other and form non-covalent interactions. It might also reduce the affinity for ERp44. The result is the secretion of compact $\mu_{s2}L_2$ species. ERp44 may help polymerization also by increasing the concentration of $\mu_{s2}L_2$ subunits in a suitable environment, possibly favoring their interactions with ERGIC-53 and/or Ero1 (Anelli *et al*, 2007; Tempio *et al*, 2021).

The "conflict of interest" of C575 in IgM assembly is only apparent. Dimerization brings the $\mu_s$tp peptides into close proximity, and non-native disulfide bonds form because of the high local concentration. These bonds might allow $\mu_{s2}L_2C575_{OX}$ subunits to avoid covalent interactions with the ER protein matrix (Reddy *et al*, 1996; Meunier *et al*, 2002), reach ER exit sites, and enter COPII vesicles with the help of ERGIC-53 (Anelli *et al*, 2007; Tempio *et al*, 2021). Then, post-ER disulfide quality control comes into play. Exploiting its mobility along the early secretory compartment (Tempio *et al*, 2021), ERp44 attacks non-native disulfides with its C29 favoring attainment of the native conformation. This system allows the perfect timing of IgM biogenesis along the early secretory compartment, ensuring that only correctly assembled oligomers are secreted.

Non-native disulfides are often formed and isomerized during oxidative protein folding (Darby & Creighton, 1993; Weissman & Kim, 1993; Cho & Collet, 2013). They can be also important steps in the biogenesis of secretory proteins, as in the case of low-density lipoprotein receptors (Jansens *et al*, 2002; Oka *et al*, 2013). The remarkable conservation of C575 and hydrophobic residues in the $\mu_s$tp implies a strong evolutionary pressure for the mechanism we describe herein. C414 bonds do not form in secretory IgM when ERp44 is absent or when the hydrophobic motif in the $\mu_s$tp is mutated. Thus, the attack of the non-native 575-575 bond by ERp44 promotes processive polymerization ultimately favoring C414 reactivity. It is tempting to speculate that this complex assembly pathway evolved to allow efficient production of secretory IgM while reducing the risk that membrane IgM antibodies form inter-subunit disulfides via C414, which would be detrimental for BCR signaling. Our preliminary data indicate that B splenocytes from mice lacking ERp44 in the B-cell compartment express surface IgM, respond to mitogenic stimulation and—as expected—secrete abundant unpolymerized IgM (TA *et al*, in preparation). Competing with BCR recognition for antigen, premature IgM secretion would be detrimental for primary immune responses. It is not surprising that also post-translational mechanisms prevent IgM secretion in B cells. No plasma-cell-specific factors have been identified so far, apart from J chains and pERp1/MZB. However, their absence does not preclude formation of the non-native bond and polymerization in HEK cells. It will be of great interest to dissect the mechanisms that mediate the differential redox fate of C575 and C414 in resting and activated B cells.

# Materials and Methods

## Cells

HEK293 cells, obtained from ATCC, and HeLa ERp44[KO] cells, obtained as described below, were cultured in Dulbecco's modified Eagle's medium (DMEM) supplemented with 10% fetal calf serum (FCS; EuroClone), penicillin–streptomycin (5 mg/ml) (Lonza), and glutamine (2mM). J558L myeloma transfectants (Sitia *et al*, 1990) and the B1.8 mouse hybridoma (Reth *et al*, 1978) were maintained in RPMI supplemented with 10% FCS, 2 mM glutamine, 1 mM Na-pyruvate, and penicillin–streptomycin 5 mg/ml. I.29μ + cells (Stavnezer *et al*, 1984) were cultured in RPMI supplemented with 10% mitogen-free FCS, penicillin–streptomycin (5 mg/ml), non-essential amino acids (1 mM) glutamine (2 mM), sodium pyruvate (1 mM), and 50 μM 2-mercaptoethanol.

## Generation of ERp44^{−/−} HeLa cells by CRISPR-Cas9

The cloning protocol by the Zhang lab (https://www.addgene.org/crispr/zhang/) was followed to generate CRISPR plasmids for ERp44. gRNA guiding sequence #218 (ATCTGAGGTCGGG-TAAGGAT) was designed with CRISPOR algorithm (http://crispor.tefor.net/crispor.py) to target exon 1 of human ERp44 genomic sequence (nucleotides 21–40 from initial ATG) generating a frameshift within the signal peptide sequence of pro-ERp44. The following pairs of oligonucleotides (sense and antisense with suitable overhangs) were purchased by Metabion: CAC CGA TCT GAG GTC GGG TAA GGAT (*gRNA218_sense);* AAA CAT CCT TAC CCG ACC TCA GATC (*gRNA218 antisense)*. Oligos were annealed and cloned into pX459 v2.0 vector (Addgene #62988) as described in (https://www.addgene.org/crispr/zhang/). This vector drives the expression of both desired gRNA and Cas9-GFP. Following antibiotic selection with puromycin cells were cloned by limiting dilution, and clone 218B1 was selected.

## Cell transfection and secretion

HEK293T and ERp44[KO] cells were transfected with jetPEI (Polyplus-transfection) following the manufacturer's recommendations. After transfection, cells were cultured for 48 h before biochemical analyses.

To analyze IgM secretion, 48 h after transfection, cells were incubated with minimal essential medium (Opti-MEM) for 4 h. Cell culture supernatants were supplemented with protease inhibitors (Roche) and treated with 10 mM N-ethylmaleimide (NEM; Sigma-Aldrich) to block disulfide interchange.

## Cell lysis and protein precipitation

Spent media were collected and concentrated with 10% v/v TCA. Cells were washed in PBS with 10 mM NEM. Cells were then lysed in radioimmunoprecipitation assay (RIPA) buffer [150 mM NaCl, 1% 4-hydroxy-3-nitrophenyl acetyl (Nonidet P-40; Sigma–Aldrich), 0.1% SDS, 50 mM Tris–HCl (pH 8.0)] supplemented with 10 mM NEM and protease inhibitors (Roche)] for 20 min on ice and postnuclear supernatants collected after centrifugation. Aliquots from cell lysates or supernatants were resolved by SDS/PAGE under reducing or non-reducing conditions, transferred to nitrocellulose, and blotted with different antibodies (i.e., goat anti-mouse IgM (μ chain) Alexa Fluor 647 (Invitrogen Molecular Probes); goat anti-mouse λ-HRP (Southern Biotech) anti-ERp44: anti-Halo-tag pAb (Promega) or Halo-tag TMR DirectLigand (Promega). Signals were acquired by Typhoon FLA 9000 (Fujifilm) and Chemidoc Imaging System (UVITEC).

### Deglycosylation of proteins

Samples were treated with endoglycosidase H (Endo-H) or PNGase-F (New England Biolabs) following the manufacturer's instructions. When non-reducing gels were to be used, DTT was omitted from all digestion buffers.

### Protein digestion and mass spectrometry analyses

To analyze the oxidative state of C575 in $\mu_{s2}L_2$ subunits, lysates from B1.8 cells were concentrated by affinity chromatography with Sepharose-bound 4-hydroxy-3-nitrophenylacetyl (NP). I.29$\mu$ + cell lysates were immunoprecipitated with rabbit anti-mouse anti-$\mu$ (Thermo Fisher) crosslinked to protein G Sepharose resin.

Purified IgM antibodies were resolved by preparative gels and stained with Coomassie blue.

Bands of interest were excised from the gel and first treated with 55 mM N-ethylmaleimide (NEM) to alkylate cysteine-free thiols; then, disulfide bonds were reduced with 10mM DTT and alkylated with 55 mM Iodoacetamide (IAA). To remove N-linked oligosaccharides was used PNGase-F and after that proteins were digested overnight with Trypsin.

Peptides were desalted on a StageTip C18 and analyzed by nLC-ESI-MS/MS on a quadrupole Orbitrap QExactive mass spectrometer (Thermo Fisher Scientific) coupled with an Easy-nLC 1000 (Thermo Fisher Scientific) with a 25 cm, 75 $\mu$m ID n-column packed in-house with ReproSil-Pur C18-AQ beads, 1.9 $\mu$m (Dr. Maisch Gmbh, Ammerbuch, Germany).

Peptide separation was achieved with a linear gradient from 95% solvent A (2% ACN, 0.1% formic acid) to 50% solvent B (80% acetonitrile, 0.1% formic acid) over 23 min and from 50% to 100% solvent B in 2 min at a constant flow rate of 0.25 $\mu$l/min, with a single run time of 33 min. MS data were acquired using a DDA top 15 method, and the survey full scan MS spectra (300–1,750 Th) were acquired in the Orbitrap with 60000 resolution, AGC target 1e$^6$, IT 120 ms. For HCD spectra, resolution was set to 15,000, AGC target 1e$^5$, IT 120 ms; normalized collision energy 28% and isolation width of 3.0 *m/z*.

### MS data analysis

For protein identification and analysis of cysteine modifications in IgM, the. Raw data were processed using Proteome Discoverer (version 1.4, Thermo Fischer Scientific). MS/MS spectra were searched with Mascot engine (version 2.6.0, Matrix Science) against the database uniprot_cp_mouse setting the parameters: enzyme: trypsin; maximum missed cleavage: 2; variable modifications: carbamidomethylation(C), oxidation (M), protein N-terminal acetylation, N-ethylmaleImide (C), N-ethylmaleimide + water (C), and deamidation (N); peptide mass tolerance: 10 ppm; MS/MS tolerance: 20 mmu. Scaffold (version Scaffold_4.3.3, Proteome Software Inc., Portland, OR) was used to validate MS/MS-based peptide and protein identifications. Peptide identifications were accepted if they could be established at greater than 95.0% probability by the Scaffold Local FDR algorithm. Protein identifications were accepted if they could be established at > 99.0% probability and contained at least 2 identified peptides. Protein probabilities were assigned by the Protein Proph*et al*gorithm (Nesvizhskii, Al *et al* Anal. Chem. 2003;75(17):4646-58).

### Data analysis by MaxQuant

To measure the intensity of peptides. Raw files were processed using MaxQuant (version 1.6.0.16) searching against the database uniprot_cp_mouse in which trypsin enzyme specificity and up to two missed cleavages were allowed; cysteine alkylation by Iodoacetamide or *N*-ethylmaleimide or *N*-ethylmaleimide + water, protein N-terminal acetylation, asparagine deamidation, and methionine oxidation were set as variable modifications. Mass deviation for MS/MS peaks was 20 ppm. The peptides and protein false discovery rates (FDR) were set to 0.01; the minimal length required for a peptide identification was six amino acids; a minimum of two peptides and at least one unique peptide were required for high-confidence protein identification.

The derived intensities of peptides with C575 of IgM in reduced form (alkylated by NEM) and in oxidized form (alkylated by IAA), normalized by IgM protein intensity were used for a rough estimation of relative peptide abundances.

### Separation of soluble IgM from membrane IgM in lysate of I.29$\mu$+ cells

I.29$\mu$ + cells were treated with or without 20 $\mu$g/ml LPS (Sigma) and lysed with Triton X-114 to separate membrane and soluble proteins. Cells were collected, washed in PBS with 10 mM NEM, and then kept for 10 min at 0°C in lysis buffer [Tris/HCl 10 mM (pH7.5), NaCl 150 mM, Triton X-114 1%, NEM 10 mM, protease inhibitors]. The postnuclear supernatant was collected after centrifugation at 0°C and incubated at 37°C for 3 min. The detergent (containing the membrane IgM) and the aqueous (containing the soluble IgM) phases were separated after a first centrifugation at room temperature for 2 min at 9,600 *g* in a benchtop centrifuge. Cold lysis buffer was added to the detergent and the aqueous phases. The two phases were left on a rotating wheel for 5 min at 0°C, then incubated other 3 min at 37°C, and centrifuged again at 9,600 *g* for 2 min at room temperature. The two phases were again separated and collected in two different tubes.

### AMS alkylation

The TX114 aqueous phases obtained from 10*10$^6$ I.29$\mu$ + cells at days 0 and 4 of LPS stimulation were fractionated on discontinuous sucrose gradients (0-5-7.5-10-12.5-15-17.5-20%) by centrifugation at 375,000 *g* for 3 h in Beckman SW55Ti rotor. Fractions containing the IgM intermediate of interest were collected, reduced with DTT, precipitated with TCA, and subjected to AMS alkylation, by resuspending the pellet in 200 mM Tris/HCl pH 8, 3% SDS, and 15mM AMS. Samples were incubated for 15 min at 37°C and then 20 min at room temperature. Alkylated $\mu_s$ chains were analyzed by Western blotting or mass spectrometry.

## Data availability

This study includes no data deposited in external repositories.

**Expanded View** for this article is available online.

## Author contributions

CG, JB, and RS designed research; CG, MRC, TA, AO, and TN performed research; CG, JB, and RS wrote the paper; all authors discussed the results and agree to the main conclusions.

## Conflict of interest

The authors declare that they have no conflict of interest.

# References

Alberini C, Biassoni R, DeAmbrosis S, Vismara D, Sitia R (1987) Differentiation in the murine B cell lymphoma I.29: individual mu + clones may be induced by lipopolysaccharide to both IgM secretion and isotype switching. *Eur J Immunol* 17: 555–562

Alt FW, Bothwell ALM, Knapp M, Siden E, Mather E, Koshland M, Baltimore D (1980) Synthesis of secreted and membrane-bound immunoglobulin mu heavy chains is directed by mRNAs that differ at their 3' ends. *Cell* 20: 293–301

Anelli T (2003) Thiol-mediated protein retention in the endoplasmic reticulum: the role of ERp44. *EMBO J* 22: 5015–5022

Anelli T, Ceppi S, Bergamelli L, Cortini M, Masciarelli S, Valetti C, Sitia R (2007) Sequential steps and checkpoints in the early exocytic compartment during secretory IgM biogenesis. *EMBO J* 26: 4177–4188

van Anken E, Romijn EP, Maggioni C, Mezghrani A, Sitia R, Braakman I, Heck AJR (2003) Sequential waves of functionally related proteins are expressed when B cells prepare for antibody secretion. *Immunity* 18: 243–253

Boes M (2000) Role of natural and immune IgM antibodies in immune responses. *Mol Immunol* 37: 1141–1149

Brandtzaeg P, Prydz H (1984) Direct evidence for an integrated function of J chain and secretory component in epithelial transport of immunoglobulins. *Nature* 311: 71–73

Brewer JW, Corley RB (1997) Late events in assembly determine the polymeric structure and biological activity of secretory IgM. *Mol Immunol* 34: 323–331

Cals MM, Guenzi S, Carelli S, Simmen T, Sparvoli A, Sitia R (1996) IgM polymerization inhibits the Golgi-mediated processing of the mu-chain carboxy-terminal glycans. *Mol Immunol* 33: 15–24

Cattaneo A, Neuberger MS (1987) Polymeric immunoglobulin M is secreted by transfectants of non-lymphoid cells in the absence of immunoglobulin J chain. *EMBO J* 6: 2753–2758

Cenci S, Mezghrani A, Cascio P, Bianchi G, Cerruti F, Fra A, Lelouard H, Masciarelli S, Mattioli L, Oliva L *et al* (2006) Progressively impaired proteasomal capacity during terminal plasma cell differentiation. *EMBO J* 25: 1104–1113

Chapuis RM, Koshland ME (1974) Mechanism of IgM polymerization. *Proc Natl Acad Sci USA* 71: 657–661

Cho S-H, Collet J-F (2013) Many roles of the bacterial envelope reducing pathways. *Antioxid Redox Signal* 18: 1690–1698

Cortini M, Sitia R (2010) ERp44 and ERGIC-53 synergize in coupling efficiency and fidelity of IgM polymerization and secretion. *Traffic* 11: 651–659

Czajkowsky DM, Shao Z (2009) The human IgM pentamer is a mushroom-shaped molecule with a flexural bias. *Proc Natl Acad Sci USA* 106: 14960–14965

Darby NJ, Creighton TE (1993) Dissecting the disulphide-coupled folding pathway of bovine pancreatic trypsin inhibitor. Forming the first disulphide bonds in analogues of the reduced protein. *J Mol Biol* 232: 873–896

Davis AC, Roux KH, Shulman MJ (1988) On the structure of polymeric IgM. *Eur J Immunol* 18: 1001–1008

Davis AC, Shulman MJ (1989) IgM - molecular requirements for its assembly and function. *Immunol Today* 10: 118–128

Feinstein A, Munn EA (1969) Conformation of the free and antigen-bound IgM antibody molecules. *Nature* 224: 1307–1309

Fra AM, Fagioli C, Finazzi D, Sitia R, Alberini CM (1993) Quality control of ER synthesized proteins: an exposed thiol group as a three-way switch mediating assembly, retention and degradation. *EMBO J* 12: 4755–4761

Giannone C, Fagioli C, Valetti C, Sitia R, Anelli T (2017) Roles of N-glycans in the polymerization-dependent aggregation of mutant Ig-μ chains in the early secretory pathway. *Sci Rep* 7: 41815

Hampe L, Xu C, Harris PWR, Chen J, Liu M, Middleditch M, Radjainia M, Wang Y, Mitra AK (2017) Synthetic peptides designed to modulate adiponectin assembly improve obesity-related metabolic disorders. *Br J Pharmacol* 174: 4478–4492

Hendrickson BA, Conner DA, Ladd DJ, Kendall D, Casanova JE, Corthesy B, Max EE, Neutra MR, Seidman CE, Seidman JG (1995) Altered hepatic transport of immunoglobulin A in mice lacking the J chain. *J Exp Med* 182: 1905–1911

Hiramoto E, Tsutsumi A, Suzuki R, Matsuoka S, Arai S, Kikkawa M, Miyazaki T (2018) The IgM pentamer is an asymmetric pentagon with an open groove that binds the AIM protein. *Sci Adv* 4: eaau1199

Jansens A, van Duijn E, Braakman I (2002) Coordinated nonvectorial folding in a newly synthesized multidomain protein. *Science* 298: 2401–2403

Källberg E, Leanderson T (2006) Joining-chain (J-chain) negative mice are B cell memory deficient. *Eur J Immunol* 36: 1398–1403

Kehry M, Ewald S, Douglas R, Sibley C, Raschke W, Fambrough D, Hood L (1980) The immunoglobulin μ chains of membrane-bound and secreted IgM molecules differ in their C-terminal segments. *Cell* 21: 393–406

Li Y, Wang G, Li N, Wang Y, Zhu Q, Chu H, Wu W, Tan Y, Yu F, Su X-D *et al* (2020) Structural insights into immunoglobulin M. *Science* 367: 1014–1017

Meunier L, Usherwood Y-K, Chung KT, Hendershot LM (2002) A subset of chaperones and folding enzymes form multiprotein complexes in endoplasmic reticulum to bind nascent proteins. *Mol Biol Cell* 13: 4456–4469

Mihaesco C, Mihaesco E, Metzger H (1973) Variable J-chain content in human IgM. *FEBS Lett* 37: 303–306

Milstein CP, Richardson NE, Dieverson EV, Feinstein A (1975) Interchain disulphide bridges of mouse immunoglobulin M. *Biochem J* 151: 615–624

Müller R, Gräwert MA, Kern T, Madl T, Peschek J, Sattler M, Groll M, Buchner J (2013) High-resolution structures of the IgM Fc domains reveal principles of its hexamer formation. *Proc Natl Acad Sci USA* 110: 10183–10188

Neuberger MS, Williams GT, Fox RO (1984) Recombinant antibodies possessing novel effector functions. *Nature* 312: 604–608

Oka OBV, Pringle MA, Schopp IM, Braakman I, Bulleid NJ (2013) ERdj5 is the ER reductase that catalyzes the removal of non-native disulfides and correct folding of the LDL receptor. *Mol Cell* 50: 793–804

Pasalic D, Weber B, Giannone C, Anelli T, Müller R, Fagioli C, Felkl M, John C, Mossuto MF, Becker CFW *et al* (2017) A peptide extension dictates IgM assembly. *Proc Natl Acad Sci USA* 114: E8575–E8584

Reddy P, Sparvoli A, Fagioli C, Fassina G, Sitia R (1996) Formation of reversible disulfide bonds with the protein matrix of the endoplasmic reticulum correlates with the retention of unassembled Ig light chains. *EMBO J* 15: 2077−2085

Reth M (1989) Antigen receptor tail clue. *Nature* 338: 383−384

Reth M, Hämmerling GJ, Rajewsky K (1978) Analysis of the repertoire of anti-NP antibodies in C57BL/6 mice by cell fusion. I. Characterization of antibody families in the primary and hyperimmune response. *Eur J Immunol* 8: 393−400

Rogers J, Wall R (1980) A mechanism for RNA splicing. *Proc Natl Acad Sci USA* 77: 1877−1879

Sannino S, Anelli T, Cortini M, Masui S, Degano M, Fagioli C, Inaba K, Sitia R (2014) Progressive quality control of secretory proteins in the early secretory compartment by ERp44. *J Cell Sci* 127: 4260−4269

Sidman C (1981) B lymphocyte differentiation and the control of IgM mu chain expression. *Cell* 23: 379−389

Sitia R, Neuberger M, Alberini C, Bet P, Fra A, Valetti C, Williams G, Milstein C (1990) Developmental regulation of IgM secretion: the role of the carboxy-terminal cysteine. *Cell* 60: 781−790

Stavnezer J, Abbott J, Sirlin S (1984) Immunoglobulin heavy chain switching in cultured I.29 murine B lymphoma cells: commitment to an IgA or IgE switch. *Curr Top Microbiol Immunol* 113: 109−116

Taylor B, Wright JF, Arya S, Isenman DE, Shulman MJ, Painter RH (1994) C1q binding properties of monomer and polymer forms of mouse IgM mu-chain variants. Pro544Gly and Pro434Ala. *J Immunol* 153: 5303−5313

Tempio T, Anelli T (2020) The pivotal role of ERp44 in patrolling protein secretion. *J Cell Sci* 133: jcs240366

Tempio T, Orsi A, Sicari D, Valetti C, Yoboue ED, Anelli T, Sitia R (2021) A virtuous cycle operated by ERp44 and ERGIC-53 guarantees proteostasis in the early secretory compartment. *iScience* 24: 102244

Thomas HI, Morgan-Capner P (1990) The avidity of specific IgM detected in primary rubella and reinfection. *Epidemiol Infect* 104: 489−497

Venkitaraman AR, Williams GT, Dariavach P, Neuberger MS (1991) The B-cell antigen receptor of the five immunoglobulin classes. *Nature* 352: 777−781

Watanabe S, Amagai Y, Sannino S, Tempio T, Anelli T, Harayama M, Masui S, Sorrentino I, Yamada M, Sitia R *et al* (2019) Zinc regulates ERp44-dependent protein quality control in the early secretory pathway. *Nat Commun* 10: 603

Watanabe S, Harayama M, Kanemura S, Sitia R, Inaba K (2017) Structural basis of pH-dependent client binding by ERp44, a key regulator of protein secretion at the ER-Golgi interface. *Proc Natl Acad Sci USA* 114: E3224−E3232

Weissman JS, Kim PS (1993) Efficient catalysis of disulphide bond rearrangements by protein disulphide isomerase. *Nature* 365: 185−188

Wiersma EJ, Shulman MJ (1995) Assembly of IgM. Role of disulfide bonding and noncovalent interactions. *J Immunol* 154: 5265−5272

Yang K, Li D-F, Wang X, Liang J, Sitia R, Wang C-C, Wang X (2016) Crystal structure of the ERp44-Peroxiredoxin 4 complex reveals the molecular mechanisms of thiol-mediated protein retention. *Structure* 24: 1755−1765